Double-Probe Measurements of Convection Electric Fields with the Injun-5 Satellite

DAVID P. CAUFFMAN AND DONALD A. GURNETT

Department of Physics and Astronomy
University of Iowa, Iowa City 52240

This paper reports on the initial results of the double-probe direct-current electric-field experiment on the low-altitude polar-orbiting Injun-5 satellite. With this experiment magnitudes of naturally occurring magnetospheric electric fields can be measured to an accuracy of ±30 mv/m, and under favorable conditions, to ±10 mv/m. At high latitudes, convection electric fields greater than 30 and sometimes greater than 100 mv/m are frequently observed in the auroral zone. A common feature of these high-latitude convection fields is the occurrence of abrupt reversals or discontinuities in the east-west convection velocity at auroral-zone latitudes. The reversals have been observed at both dawn and dusk local times and at magnetically conjugate points in both hemispheres. For dusk-dawn local times, these reversals correspond to an east-west flow away from the sun on the high-latitude side of the reversal and toward the sun on the low-latitude side. Over the polar region above the auroral zone the convection fields are usually not greater than ±30 mv/m, in contrast to the larger field magnitudes observed at the auroral zone. At the boundary of the plasmapause and the light ion trough small 10- to 20-mv/m electric-field perturbations are sometimes observed, corresponding to generally westward convection outside the plasmasphere. At high altitudes, above about 1500 km, over the auroral-zone and polar-cap regions, irregular electric-field 'noise' with amplitudes from 10 to 30 mv/m is often observed. Among the possible explanations of the high-altitude electric-field noise is the presence of significant (>0.5 mv/m) electric fields parallel to the geomagnetic field. The results presented are consistent with measurements made by using the barium cloud drift technique. The observed convection is also compared with models of magnetospheric structure and with models of substorms and auroras.

The importance of electric-field measurements for studying the convection of plasma in the magnetosphere has been recognized for a number of years [*Dungey,* 1961; *Axford and Hines,* 1961; *Piddington,* 1962; *Boström,* 1967; *Axford,* 1969]; however, only recently have techniques been developed for the measurement of magnetospheric electric fields. These techniques include (1) observations of the drift of artificial barium cloud releases [*Haerendel et al.,* 1967; *Föppl et al.,* 1968; *Wescott et al.,* 1969], (2) direct probe measurements made by using rockets and satellites [*Mozer and Bruston,* 1967; *Fahleson et al.,* 1970; *Heppner et al.,* 1968; *Gurnett,* 1970; *Maynard and Heppner,* 1970; *Potter,* 1970], (3) subionospheric electric-field measurements with high-altitude balloons [*Mozer and Serlin,* 1969], and (4) various other more indirect methods such as observations of whistler-duct motions [*Carpenter,* 1970], and charged-particle energy spectrum observations [*Van Allen,* 1970]. This paper reports on initial results from the double-probe direct-current electric-field experiment on the low-altitude (677 to 2528 km) polar-orbiting Injun-5 satellite. Detailed statistical analyses are underway and will be published when all the available data are analyzed.

DESCRIPTION OF THE EXPERIMENT

The electric-field sensors on Injun 5 consist of two conducting spheres 20.3 cm in diameter mounted on booms with a center-to-center distance between the spheres of 2.85 meters. The spacecraft is magnetically oriented by a bar magnet within the spacecraft such that the electric antenna axis (*y*-axis of the spacecraft) is maintained approximately perpendicular to the geomagnetic field. Typically the maximum magnetic alignment errors are less than about 10° to 15°. The dc electric-field experiment is therefore primarily sensitive to the electric field perpendicular to the geomagnetic field.

The potential difference between the two spheres is determined every 4 sec by using a high-input impedance differential amplifier lo-

cated in the main spacecraft electronics. The input impedance of the differential amplifier is 20 megohms from each sphere to the spacecraft body. This input impedance is much larger than the sheath resistances generally encountered in the Injun 5 orbit. To verify that the sheath resistance is small compared with the input impedance of the differential amplifier, the average ac impedance of the two spheres is determined every 30 sec by differentially driving the spheres with a constant-amplitude ac current source and measuring the resulting ac potential difference between the spheres. Details of the Injun 5 dc electric-field experiment are given by *Gurnett et al.* [1969].

The theory of operation for the double-probe type of electric-field antenna used on Injun 5 has been discussed by *Fahleson* [1967] and T. Aggson (unpublished data, 1966). An equivalent circuit model of the coupling of the probe system to the plasma is shown in the bottom diagram of Figure 1. In this model the voltage sources $E(l/2)$ and $E(-l/2)$ represent the plasma potential at the center of the two spheres, and V_s is the equilibrium voltage across the plasma sheath surrounding the spheres when the amplifier current is zero. The resistance R_s is the effective small-current resistance of the plasma sheath and accounts for the voltage drop across the plasma sheath due to the nonzero amplifier current. Expressions for R_s and V_s are given by *Fahleson* [1967] in terms of the plasma parameters and the antenna dimensions. The resistance $R_B = 20$ megohms in the equivalent circuit of Figure 1 represents the input resistance of the differential amplifier. Subscripts plus and minus are used to designate quantities associated with the $+y$ and $-y$ axis spheres, respectively. The sheath thickness is normally small compared with the antenna length. The effective length, l, of the antenna will therefore be equal to the physical sphere separation distance. From the circuit diagram it can be readily shown that the measured potential difference between the spheres is given by

$$\Delta V_M = -(E_y/2) \cdot \left[\frac{1}{1 + (R_{s+}/R_{B+})} + \frac{1}{1 + (R_{s-}/R_{B-})}\right] + \left[\frac{V_{s+}}{1 + (R_{s+}/R_{B+})} - \frac{V_{s-}}{1 + (R_{s-}/R_{B-})}\right] \quad (1)$$

If the sheath voltages are the same for both spheres, $V_{s+} = V_{s-}$, and the sheath resistances are small compared with the differential amplifier input impedance ($R_s \ll R_B$), the y component of the electric field is directly proportional to the potential difference between the spheres,

$$E_y = -\frac{\Delta V_M}{l} \quad (2)$$

Operation of Electric Antenna System in Orbit

The E_y electric field observed for a complete Injun-5 orbit is shown in Figure 2, as determined from the sphere potential difference by using equation 2. This orbit was selected for discussion because it illustrates a variety of 'instrumental' effects that must be eliminated before the naturally-occurring magnetospheric electric field can be determined. At middle and low latitudes, where the ionospheric plasma is expected to corotate with the earth [*Axford*, 1969], only the $\mathbf{V}_s \times \mathbf{B}$ electric field arising from the satellite velocity $\mathbf{V}_s$ through the ionosphere should be observed. The systematic sinusoidal variation evident in the measured electric field in Figure 2, with a period of about 20 min, is caused by the antenna rotation in the $\mathbf{V}_s \times \mathbf{B}$ electric field. The dashed lines in Figure 2 are the positive and negative limits of the $\mathbf{V}_s \times \mathbf{B}$ field as computed from the satellite orbit, in a coordinate system corotating with the earth. Discounting the spacecraft wake and shadow effects indicated in Figure 2, the maximums and minimums in the observed E_y electric field at middle and low latitudes are observed to fit the dashed $|\mathbf{V}_s \times \mathbf{B}|$ envelope to within about 50 mv/m. This difference is primarily due to asymmetrical sunlight shadowing of the spheres by the supporting booms.

As discussed by *Fahleson* [1967], asymmetrical shadowing causes unequal sheath voltages ($V_{s+} \neq V_{s-}$) by reducing the photoelectron current to the shadowed probe. In this case the second term in equation 1 will contribute to the measured sphere potential difference. The additional contribution due to boom shadowing of the probes varies slowly on a time scale comparable with the satellite rotation period. For the dawn-dusk orbit illustrated in Figure 2, the maximum boom

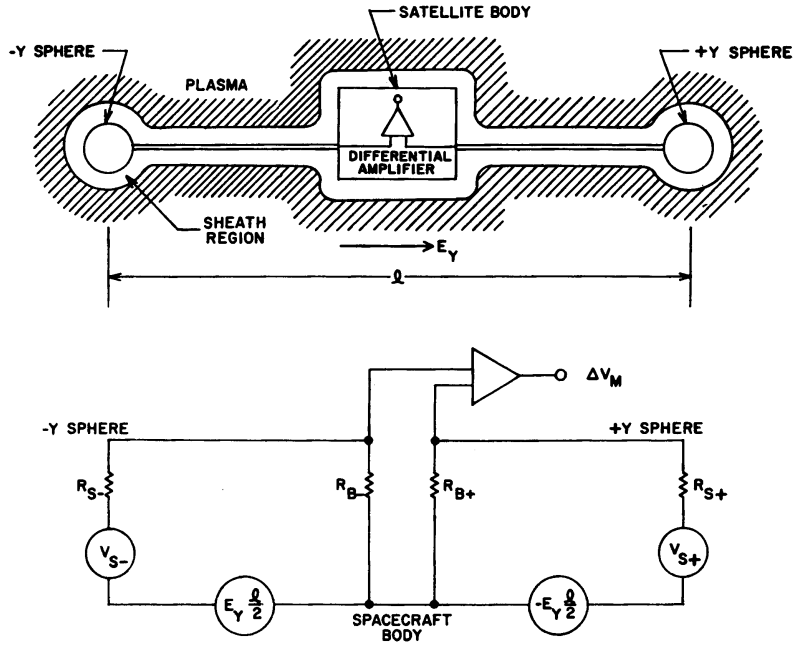

Fig. 1. Top: schematic illustration of the plasma sheath around the spacecraft and electric probes. Bottom: equivalent circuit of the probe-plasma system.

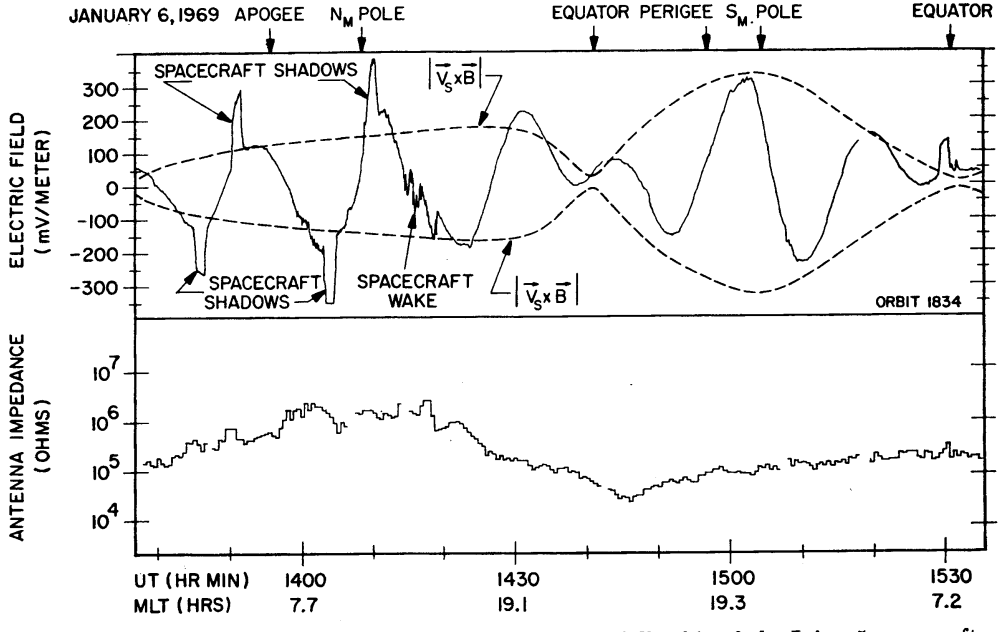

Fig. 2. Electric field $E = -(\Delta V_M/l)$ measured for one full orbit of the Injun-5 spacecraft, compared with calculated values of $|\mathbf{V}_s \times \mathbf{B}|$. Variations in the resistance of the plasma sheath around the antennas are shown in the bottom plot.

shadowing occurs when the antenna axis is aligned parallel or antiparallel to $\mathbf{V}_s \times \mathbf{B}$. Since the direction of $\mathbf{V}_s \times \mathbf{B}$ reverses between the northern and southern hemisphere, the boom shadowing error adds to $\mathbf{V}_s \times \mathbf{B}$ in one hemisphere and subtracts in the opposite hemisphere. This explains why the measured E_y 'overshoots' the computed $\mathbf{V}_s \times \mathbf{B}$ limits in the northern hemisphere and 'undershoots' by a similar amount in the southern hemisphere.

The abrupt jumps in the sphere potential difference labeled 'spacecraft shadow' in Figure 2 are due to the change in the photoelectron emission of one of the spheres as the sphere passes through the sunlight shadow of the spacecraft body. Sunlight shadowing effects caused by the spacecraft body are usually easy to identify because of their distinctive characteristics and predictable occurrence.

Perturbations due to a wake from the spacecraft body have been observed in the Injun 5 dc electric-field data. An example of a large wake effect is shown in Figure 2. As discussed in detail by *Cauffman and Gurnett* [1971] and *Cauffman* [1971], these perturbations occur when a sphere develops a photoelectron sheath in the region of reduced electron density in the spacecraft velocity wake. Since the resistance of the photoelectron sheath is greater than the resistance of the normally-occurring positive-ion sheath, wake effects occur only when the sheath resistance is very large. Wake effects may be eliminated by discarding data when the impedance exceeds 10^6 ohms while a sphere is in the wake region.

The bottom plot of Figure 2 shows the electric antenna impedance at a frequency of 30 Hz for an entire orbit. The impedance at this frequency is observed to be almost purely resistive [*Gurnett et al.*, 1969] and is believed to be almost entirely due to the plasma sheath surrounding the spheres. Typically the impedances observed in flight are less than 1 megohm, so corrections to the electric-field determination due to the finite differential amplifier input impedance (see equation 1) are usually negligible. If the sheath resistance exceeds 1 megohm, it is necessary to consider the errors caused by the differential amplifier current and the possible occurrence of wake effects. *Cauffman* [1971] discusses in detail the error analysis performed for the Injun-5 dc electric-field experiment.

DATA REDUCTION PROCEDURE

To separate naturally occurring electric fields from instrumental effects, it is necessary to subtract the $\mathbf{V}_s \times \mathbf{B}$ electric field and other known errors from the measured electric field. In the preceding section the procedure used to identify wake and spacecraft shadow effects was described. The component of the $\mathbf{V}_s \times \mathbf{B}$ electric field parallel to the antenna axis, $\hat{y} \cdot \mathbf{V}_s \times \mathbf{B}$, is also easily calculated. The only major problem remaining is to correct for the smooth long-term variations caused by asymmetrical boom shadowing. While boom shadowing is understood in principle, in practice this error cannot be calculated with sufficient accuracy to be useful because of uncertainties in the various plasma parameters involved.

The procedure that has been adopted for subtracting $\hat{y} \cdot \mathbf{V}_s \times \mathbf{B}$ and the boom shadowing error is the following: a smooth curve E_s is handdrawn through the measured electric field subject to the following requirements. (1) It has a sine wave shape that is qualitatively the same as the computed $\hat{y} \cdot \mathbf{V}_s \times \mathbf{B}$ field. (2) The modulation amplitude and phase are adjusted to provide a good fit at low latitudes where no convection electric fields are expected. (3) In cases of uncertainty the curve is drawn closer to the average measured field.

This procedure considers both $\hat{y} \cdot \mathbf{V}_s \times \mathbf{B}$ and the smooth changes due to boom shadowing. In cases of uncertainty the residual electric field, $E_R = E_M - E_S$, will in general underestimate the actual convection electric field. If natural electric fields occur that are small and uniform for times comparable with the rotation period of the spacecraft, they will unfortunately but unavoidably be subtracted out by this procedure and will not appear in E_R. Because of the unknown spatial variations in the plasma parameters affecting the boom shadowing, the absolute values of E_S and E_R cannot in general be determined to better than about ± 30 mv/m. However, variations in the residual electric field that occur with periods much less than the satellite spin period are considered significant if their magnitude exceeds 10 mv/m. In favorable cases, when the spacecraft rotation period is very long (>1 hour) and the electric antenna orientation is such as to eliminate boom shadowing, the electric field can be determined to an absolute accuracy of ± 10 mv/m.

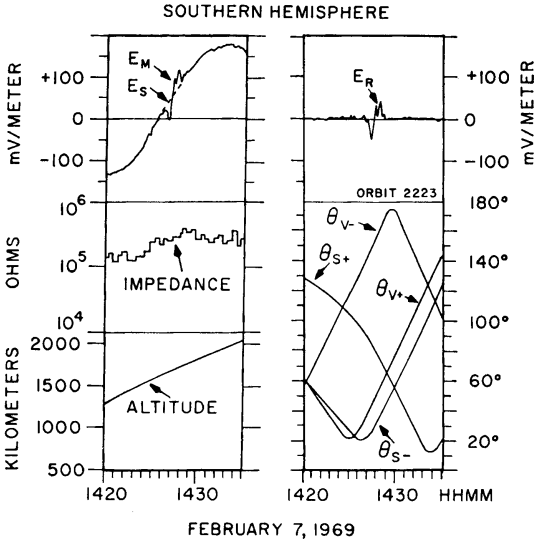

Fig. 3. Example of a sudden reversal in the convection electric field. E_M is the measured electric field; E_s is the $\hat{y}\cdot\mathbf{V}_s\times\mathbf{B}$ electric field; and $E_R = E_M - E_s$ is assumed to be the convection electric field. Antenna orientation angles and sheath impedance (see text) are used to verify that the reversal is not an instrumental effect.

Figure 3 illustrates the data reduction procedure used to determine the residual electric field, E_R, for a typical case. The solid curve is the measured electric field, E_M, and the dashed curve, E_S, is the smooth curve drawn to best approximate the $\mathbf{V}_s\times\mathbf{B}$ field and the boom shadowing error. The residual electric field, $E_R = E_M - E_S$, has an abrupt reversal of approximately ± 50 mv/m at 1428 UT. The sheath impedance is less than 10^6 ohms. The angles between the probes and the sun vector, θ_s, and between the probes and the satellite velocity vector, θ_v, verify that for this event neither probe was in a wake or a shadow. Hence this electric-field reversal is assumed to be due to a convection electric field.

Axford [1969] has explained that at Injun-5 altitudes the conductivities are such that a dc electric field is related to the convection velocity $\mathbf{V}_c$ of the plasma by the equation

$$\mathbf{V}_c = (\mathbf{E}\times\mathbf{B}/B^2) \qquad (3)$$

The convection velocity component associated with the residual electric field E_R shown in Figure 3 is illustrated on a polar diagram of magnetic local time versus invariant latitude in Figure 4. Each arrow represents the measured component of the convection velocity computed by using equation 3. The length of the arrow is proportional to the maximum magnitude of V_c during the preceeding 30 sec and the direction of the arrow is in the direction of the convection velocity sensed. The base of each arrow, or the location of each dot, gives the satellite position at half-minute intervals. It must be emphasized that the arrow represents only the component of the convection velocity detected; it does not represent the vector direction of the convection velocity, since only one component is measured. The electric-field reversal shown in Figure 3 appears in Figure 4 as a reversal in the east-west component of the convection velocity. Because of the orientation of the spacecraft during this event, the north-south component of the convection velocity cannot be determined.

Convection velocity variations determined for intervals smaller than the spin period of the spacecraft and for cases with favorable antenna orientations and long spin periods are believed to be uncertain by about 0.25 km/sec (using this data reduction procedure) and, as in the case of E_R, represent a lower limit. Uniform convection velocities for times comparable to the satellite spin period are not expected to be detectable if the convection velocity is less than about 0.75 km/sec, because slowly varying electric fields are eliminated in the data reduction procedure. Convection magnitudes computed to be less than ± 0.25 km/sec are represented by dots on the polar diagrams.

Characteristics of Observed Electric Fields

On virtually every orbit of the satellite, significant residual electric fields not attributable to any known instrumental effect are observed. These electric-field effects, which are assumed to be due to plasma convection phenomena, are only observed at middle and high latitudes. Above 60° invariant latitude, electric fields with fluctuations greater than 10 mv/m are observed on nearly every pass, and occasionally magnitudes greater than 100 mv/m are observed. Many of these fluctuations take the form of discrete auroral-zone events called electric-field 'reversals,' discussed in Section *A* below. Small changes sometimes observed at the plasmapause are discussed in Section *B*. Other electric field variations, irregular and broader in extent, are

classified as 'noise' and are discussed in Section C.

A. *Auroral-Zone Field Reversals*

A phenomenon that is observed to occur only in the auroral zone, and on approximately 36% of the auroral-zone crossings studied, is an abrupt reversal in the residual electric field, E_R, and the convection velocity, V_c. These events are the easiest of the observed phenomena to study both because the signature of a reversal cannot arise owing to a spurious shadow, and because the over-all magnitude cannot be changed by an error in drawing E_s. Any uncertainty is thus confined to where the electric field or convection velocity crosses zero; the peak-to-peak magnitude is unaffected by the data reduction.

Figure 5 shows three reversals occurring at dawn on different days of January 1969. The convection directions for the three are typical in showing antisunward flow at higher latitudes and sunward flow at lower latitudes. In all three examples the reversal occurs at about 75° invariant latitude (INV). Reversals usually occur in the auroral zone between 70° and 80° INV and are not observed over the polar cap or at middle and low latitudes. As illustrated in Figure 5, electric-field magnitudes are generally larger at dawn than at dusk.

Figure 6 shows a striking example of reversals that occur at conjugate ends of the same magnetic-field lines. The polar diagrams represent opposite hemispheres 1 hour (one-half orbit) apart. On the dawn side, in the northern hemisphere, a reversal occurs at ~74° INV. In the opposite hemisphere, the reversal occurs at 70° INV, again at ~3.5 hours MLT. The electric fields (not shown) for these reversals show several oscillations with ~20-sec periods on the low-latitude side of each of the three reversals. On the dusk side of Figure 6 another, smaller pair of conjugate reversals may be seen at 75° INV and ~15.5 hours MLT.

Special mention should be made of the observation at 1643 UT in Figure 6. Here, because the satellite rotates, only the north-south component of convection is being measured. Simultaneously, the magnitude of convection measured becomes equal to zero, and afterward again becomes nonzero. Both before and after, the convection is determined to have eastward components. This event is interpreted to mean that the true convection direction was eastward, with no north-south component. One hour later (at 1730 UT) at the magnetically conjugate location, only the east-west component was being measured, and large eastward convection is observed.

Figure 7 depicts an example of pairs of convection reversals occurring on both sides of the polar cap at about 75° INV, for three successive passes over the north polar cap. A large zone of

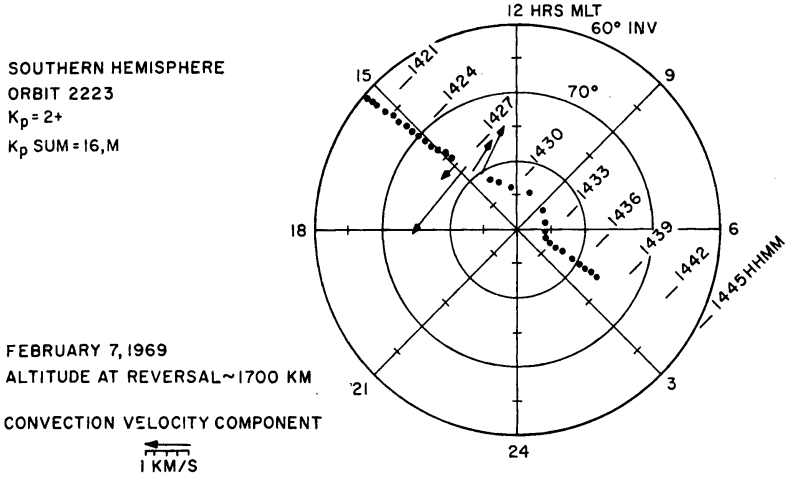

Fig. 4. Convection velocity components inferred from $\mathbf{v} = \mathbf{E}_R \times \mathbf{B}/B^2$ for the electric-field reversal shown in Figure 3. The arrow represents only the convection velocity component sensed and does not represent the vector direction of the convection velocity since only one component is measured.

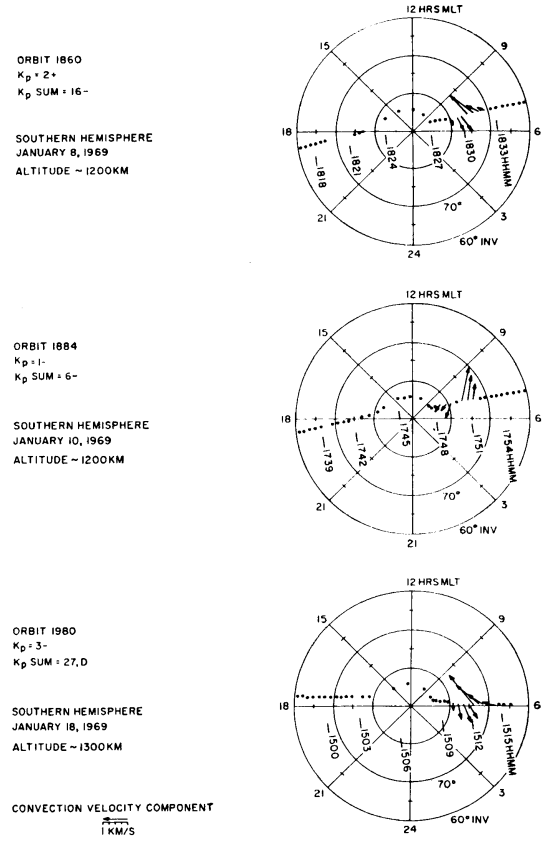

Fig. 5. Convection velocity reversals inferred from dc electric-field measurements on three different days of January 1969. The reversals occur at dawn and all have sunward (antisunward) components on the low (high) latitude side of the reversal.

convection appears to be directed across the center of the polar cap from ~1000 toward ~2200 hours MLT in the top diagram. At 1930 UT in the middle diagram the 0400–1600 hours MLT component of convection is being measured, and no electric field is measured. This does not rule out the possibility that convection in the 1000–2200 direction persisted at 1930 UT. Some of the variation in velocity magnitude between passes in Figure 7 may be ascribed to the different orientations of the satellite. However, a close examination of the convection zones at 1924 and 2121 UT, for example, shows that in the 2 hours between passes the magnitude of the eastward convection component changes significantly, the width of the zone changes, and the invariant latitude of the reversal shifts by several degrees. Thus the time scales of the phenomena in this example are shorter than the 2 hours between passes, although the over-all pattern persists.

Figures 5, 6, and 7 illustrate the persistent occurrence of reversals in the east-west direction of the convection in the auroral zone. In most of these cases the primary convection pattern is limited to a region several degrees in latitude on either side of the reversal with sunward convection generally observed on the low-latitude

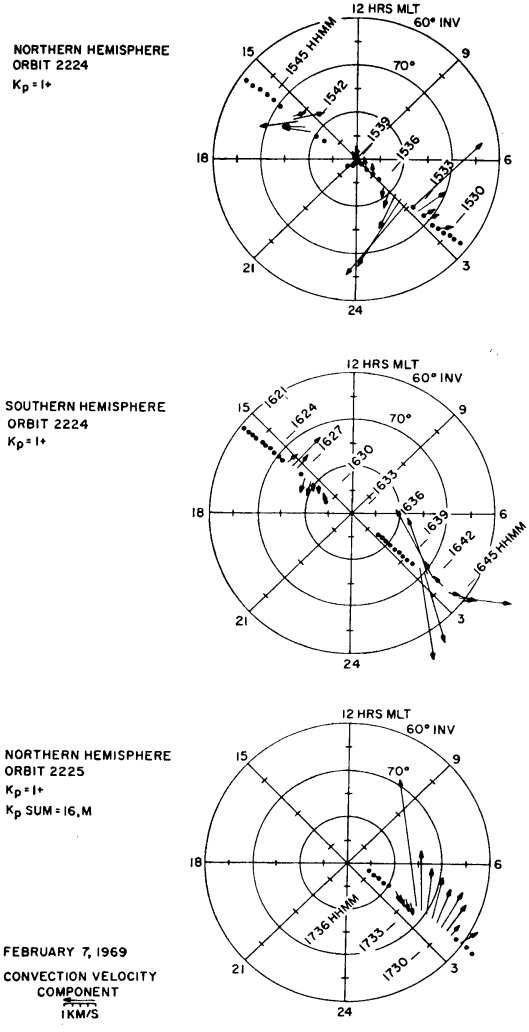

Fig. 6. Convection velocity reversals observed to occur on conjugate ends of the same geomagnetic field lines, 1 hour apart. The 5 reversals shown, 3 at 0300 MLT and 2 at 1500 MLT, all possess sunward (antisunward) convection components on the low (high) latitude side of the reversals.

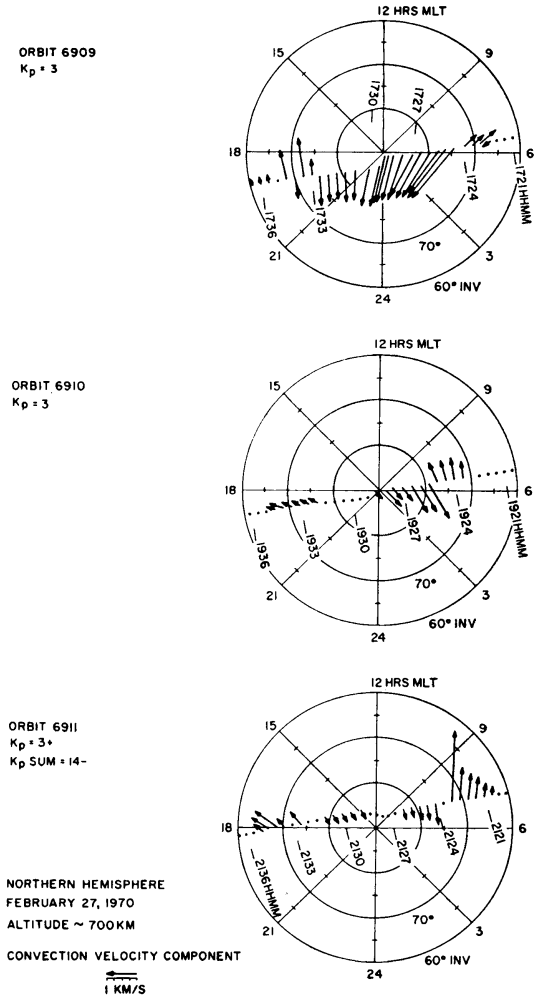

Fig. 7. Pairs of convection velocity reversals observed at dawn and dusk MLT on 3 successive passes over the northern polar cap. The existence of a temporary antisunward convection zone across the polar cap is suggested by the data on the top figure.

side of the reversal and antisunward convection on the high-latitude side of the reversal. For about 14% of reversals, generally antisunward, >0.75 km/sec convection is observed over the polar cap. The ±30-mv/m uncertainty in the absolute measurement prevents us from determining whether weaker, steady convection is common across the polar cap. For several cases with slow rotation and favorable antenna orientations, the convection electric field over the polar cap region has been observed to be less than 10 mv/m ($V_c < 0.25$ km/sec). Broad convection zones with velocities as high as 2 km/sec over the polar region, such as those evident at 1727 UT in Figure 7, occur rarely.

The dependence of the occurrence of reversals on magnetic activity is presently under study. The examples of reversals shown in Figures 4, 5, 6, and 9 occurred when magnetic activity as measured by *Kp* was relatively quiet.

Figure 8 shows two oppositely directed electric-field zones separated by a broad region of zero electric field, rather than by a sharp reversal. This pass is interesting because the satellite was not rotating, and the electric antenna axis was parallel to the velocity vector, as illustrated in Figure 9. The orientation is fortunately such as to exclude all shadow and boom effects. Under this (rather rare) set of circumstances, and assuming that the electric fields are a spatial effect, the potential across the polar cap may be integrated directly from the electric field:

$$\phi = -\int \mathbf{E} \cdot d\mathbf{s} \qquad (4)$$

The potential, plotted in the top of Figure 8, reaches 44,000 volts in about 2500 km. The polar diagram in Figure 9 shows the convection velocity components implied by the measured electric-field zones. Only the sunward/antisunward convection component is measured. The anti-

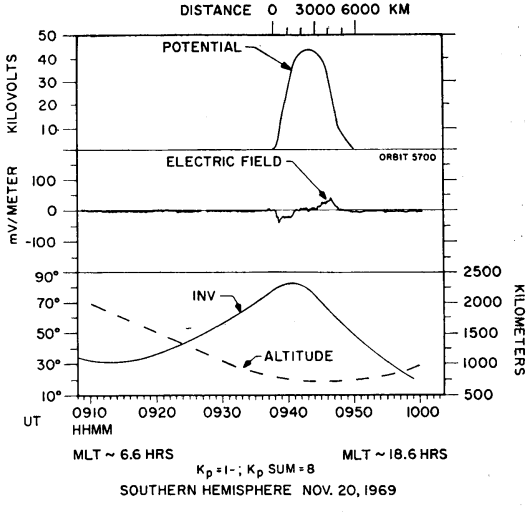

Fig. 8. Electric field measured parallel to the satellite path for a southern polar-cap pass at low altitude. The potential $\phi = -\int \mathbf{E} \cdot d\mathbf{s}$ reaches 44,000 volts in 2500 km.

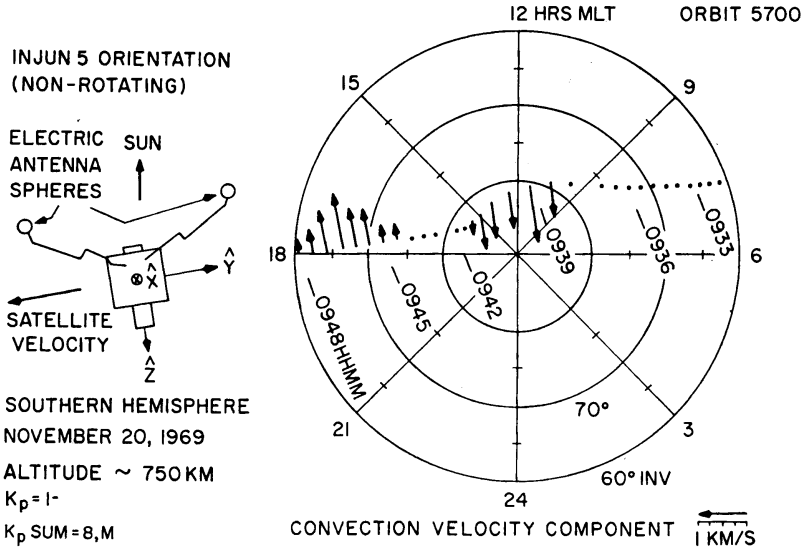

Fig. 9. Convection velocity components corresponding to the electric fields shown in Figure 8. The spacecraft orientation, as shown, is such that only the 0100–1300 MLT component is measured, since the satellite was not rotating for this pass. Sunlight shadows of the spacecraft body or booms on the spheres cannot occur for this orientation.

sunward flow above 75° INV and sunward flow below 75° INV are consistent with the convection directions shown in Figures 5, 6, and 7.

Not all electric-field reversals occur on time scales of minutes. Figure 10 shows a reversal that changes from minimum to maximum (117 mv/m) in 8 sec. The electric field shown in this example was measured every 4/30 sec. As the $\hat{y}$ axis at this time was aligned parallel to $\mathbf{V}_s$, the potential may again be found as indicated by equation 4. The top of Figure 10 shows the potential obtained, which reaches 3600 volts in less than 100 km.

The examples of reversals in Figures 4 and 10 have sunward convection at higher latitudes, thus showing that exceptions to the general pattern described above do occur.

Summary. Abrupt reversals, or discontinuities, occur in the north-south convection electric field on about 36% of auroral-zone crossings. Electric fields of >30 and sometimes >100 mv/m generally occur within several degrees INV on either side of a reversal. Reversals are observed at both dawn and dusk local times and at magnetically conjugate points in both hemispheres. For dusk-dawn local times, electric fields associated with reversals correspond to an east-west convective flow of thermal plasma away from the sun on the high-latitude side of a reversal and toward the sun on the low-latitude side. Over the polar region the convection electric fields are usually smaller than ±30 mv/m. This experiment cannot determine whether electric fields smaller than ±30 mv/m are common over the polar cap. However, the largest convection velocities typically occur near the auroral zone, not over the polar cap.

B. *The Plasmapause Boundary*

Several plasmapause crossings have been investigated to determine if any changes occur in the plasma convection velocity as the satellite crosses the boundary of the plasmapause and the light ion trough [*Carpenter,* 1966; *Taylor et al.,* 1969]. The plasmapause boundary can be identified in the Injun 5 data from (1) the characteristic 'lower hybrid resonance (LHR) breakup' effect commonly found in the VLF electric-field data at the plasmapause boundary [*Carpenter et al.,* 1968], (2) the characteristic increase in the sheath resistance at the plasmapause boundary, and (3) the change in the electron density as measured directly by the AFCRL electron-density measurement on Injun 5. Unfortunately, for the Injun-5 orbit these plasmapause indicators are not always present, so a unique identification of the plasmapause location is possible for only

a small fraction of the available data, primarily at altitudes above 2000 km during local night. Only 8 instances have been investigated at the present time for which the plasmapause location can be clearly and unambiguously identified and for which shadows cannot occur on the electric antennas. Of these, 5 crossings have small (10–20 mv/m) but clearly distinguishable perturbations in the residual electric field at the plasmapause boundary.

An illustration of one such plasmapause crossing is shown in Figure 11. Here the plasmapause crossing, from the plasmasphere into the trough region, occurred at about 08h 06m 15±15s UT, as shown by the increase in sheath resistance at this time. The dc electric field varies smoothly as the satellite crosses the plasmapause, with no evidence of the large-amplitude electric-field variations observed at higher latitudes. A small shift in the dc electric field is evident, however, shortly after crossing the plasmapause boundary. In this case, the antenna axis is aligned north-south so that the east-west component of the convection velocity is being detected. By extrapolating the smooth variation of the observed electric field from low latitude into the trough region (dashed line in Figure 11), the discontinuity in the convection electric field at the plasmapause boundary can be estimated to be about 15 mv/m. If the plasma within the plasmapause boundary is corotating with the earth, then the convection in the trough region is westward with a velocity of about 0.5 km/sec relative to a frame of reference corotating with the earth.

All of the 5 plasmapause crossings observed with significant electric-field effects at the boundary occurred in the local time range from 0000 to 0500 hours MLT. The direction of the convection velocity component measured in these 5 crossings was as follows: 3 west, 1 northwest, and 1 south. The magnitude of the change in electric field detected in all these crossings was small, 10 to 20 mv/m, and close to the resolution limit of the instrument and the data analysis technique used.

Discussion. The possibility that these small perturbations in the dc electric field near the plasmapause boundary could be caused by a change in the sheath characteristics rather than a real electric field has been investigated in detail. Neither errors caused by the change in the sheath resistance nor errors caused by an imbalance in the parameters affecting the sheath voltages of the two spheres are capable of producing the observed effect. Since no other instrumental effect is known that could account for the observed potential changes, it is concluded that these plasmapause electric-field effects are due to a change in the plasma convection at the plasmapause boundary.

C. *High-Latitude Electric-Field Noise*

At invariant latitudes greater than 60°, electric-field 'noise' is nearly always observed. This noise consists of rapid fluctuations of the observed electric field, with time scales generally less than 60 sec and amplitudes up to 150 mv/m. An example of this type of electric-field noise is illustrated in Figure 12. Some of the general characteristics of this electric-field noise are summarized below.

1. There is an apparent seasonal effect, with larger noise amplitudes occurring over the winter polar region, as evident in the example shown in Figure 12.
2. The noise usually has a fairly well-defined low-latitude limit at about 58° to 62° INV. When the amplitude of the noise is very low, however, the noise may not be observable below about 70° INV.
3. When the noise amplitudes are very low, the invariant latitude at which the fluctuations are largest is nearly always at about 70° to 75°, in the auroral zone.
4. The amplitude of the noise is strongly dependent on altitude, with larger noise levels observed at higher altitudes.
5. The amplitude of the noise is also related to the sheath resistance, to the extent that when $R_s < 10^6$ ohms, fluctuations rarely exceed 50 mv/m and are more typically 10 mv/m in amplitude, whereas, when $R_s > 10^6$ ohms, the noise amplitudes may exceed 150 mv/m, but are more typically about 30 mv/m in amplitude.
6. The noise amplitude is also related to the electron density in that the large noise levels are generally observed in regions of low electron density.

Because of the interdependence of the electron density, sheath resistance, season, satellite position, and possibly other factors, it is difficult to determine which factors are most signifi-

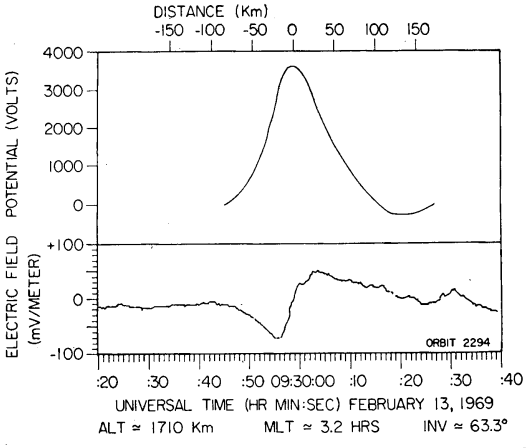

Fig. 10. Example of a very rapid reversal in the north-south electric field. The potential $\phi = -\int \mathbf{E} \cdot d\mathbf{s}$ reaches 3600 volts in less than 100 km.

cant in controlling the noise amplitude. Since spacecraft-wake effects also occur at high latitudes and high sheath resistances, large electric-field fluctuations are usually observed superimposed on the sphere potential perturbations due to the spacecraft wake. The noise does not appear to be related to the spacecraft-wake effect, however, because the noise is present with essentially the same amplitude both when the sphere is inside and when it is outside the wake region.

Discussion. The dc electric-field noise may well be due to magnetospheric convection, and possibly to small-scale vortices or turbulence. If so, the altitude-dependence of the noise amplitude provides evidence for dc electric fields parallel to the geomagnetic field. Because the noise amplitudes are typically 30 mv/m or more at apogee, but are usually negligible by comparison at perigee over the same region, there must be a potential drop on the order of 30 mv/m × (typical scale length ≃30 km) = 900 volts between apogee (2528 km) and perigee (677 km). A lower limit on the corresponding parallel electric field would therefore be about 0.5 mv/m.

Although unbalanced fluctuations in the sheath potentials, induced by electron-density or temperature variations, were initially thought to be a possible explanation of the high-latitude electric-field noise, a recent detailed investigation by *Cauffman* [1971] indicates that this process is not occurring. In particular, (1) a

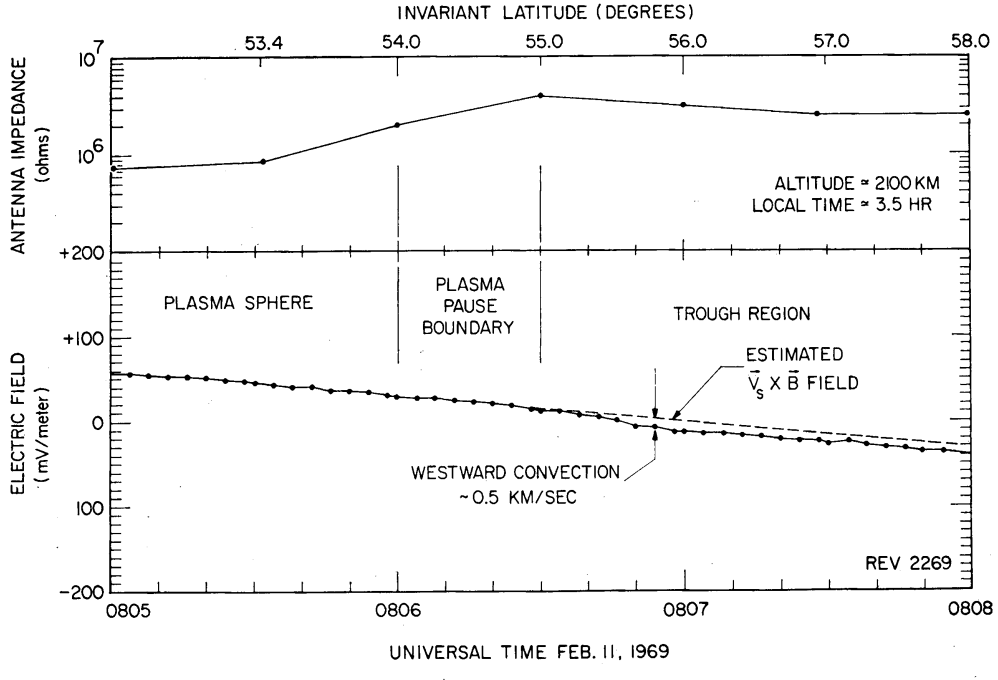

Fig. 11. Example of a small electric-field change observed near the boundary of the plasmapause and the light-ion trough.

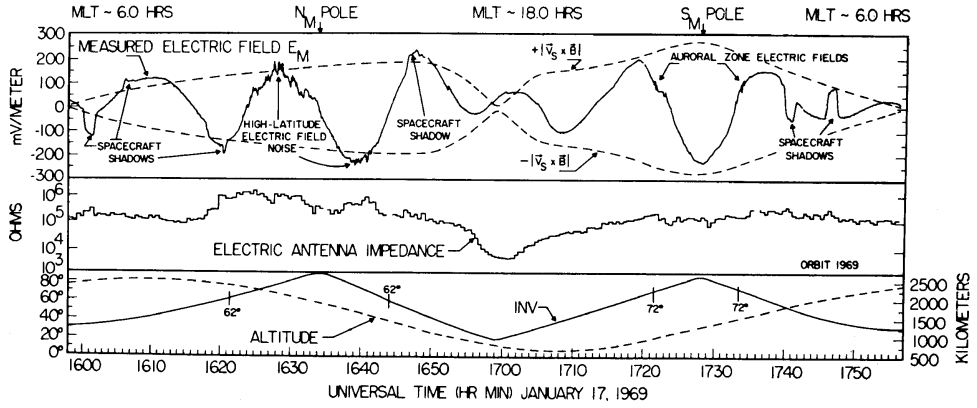

Fig. 12. Example of electric-field noise observed across the polar caps for a full orbit during January 1969. The noise amplitudes are largest over the winter pole and at high altitudes where the sheath resistances are also large.

detailed comparison of the electric-field noise with data from the AFCRL experiment on Injun 5, which measures a quantity proportional to $N_e(T_e)^{1/2}$, reveals no significant correlation; and (2) a comparison of the electric-field noise fluctuations with sheath resistance variations (R_s is proportional to T_e, but is measured only every 30 sec) also reveals no consistent correlation on the time scale being considered.

An alternative explanation is that the noise represents detection of waves generated by the spacecraft itself at high altitudes through some unknown process.

Conclusions

Comparison with other measurements. Haerendel and Lüst [1970] summarize recent results of measurements of plasma convection by the barium cloud drift technique. The requirement of twilight conditions restricts barium cloud measurements to the midnight sector and invariant latitudes generally below 70°. At local times nearer dawn, however, eastward drifts are observed, and near dusk, westward drifts. These directions are entirely consistent with the 'sunward' convection reported in this paper at dawn and dusk at comparable latitudes. Several cases of clouds reversing their drift directions have been reported. Furthermore, the magnitudes of convection velocities we observe are consistent with, for instance, those quoted by *Wescott et al.* [1969], who report intensities of 10–130 mv/m. These authors also report that large irregularities in the electric field exist most of the time.

Auroral-zone electric-field reversals also appear in Ogo-6 dc electric-field data (J. P. Heppner, private communication, 1971). These data also show the irregular variations we have called 'noise' (see Figure 2 of *Maynard and Heppner* [1970]).

Further independent confirmation of the existence of a reversal in the dc electric field at the auroral zone is provided by the anticorrelation of polar-cap and midlatitude electric fields measured with low-altitude balloons by *Mozer and Manka* [1971].

Observations of sharp boundaries in the plasma convection pattern at the plasmapause boundary have also been reported by *Haerendel and Lüst* [1970].

Comparison with magnetospheric models. Dungey [1961] suggested that the solar magnetic field could merge with the earth's magnetic field in an 'open' magnetospheric model. Field lines merged at the bow of the magnetosphere would be pulled across the polar caps by the solar wind and would reconnect on the earth's night side. Consequently there would be a return flow of field lines to the sunward side of the earth at lower latitudes. As charged particles would remain attached ('frozen') to field lines except near reconnection regions, bulk motion, or convection, of the magnetosphere would result. The measurements presented here of dc electric fields related directly to plasma convection indicate that $\gtrsim$0.75-km/sec antisolar convection flow across the polar caps is not a normal feature of the magnetosphere. Figures 7 and 9 indicate that such a convective flow does

occasionally occur, but the observed velocities are much less than would be expected from a geometrical reduction of the solar-wind velocity to the Injun-5 satellite altitude.

Axford and Hines's [1961] 'closed' magnetospheric model more explicitly suggested convection across the polar cap with return flow at the auroral zone, but used 'viscous interaction' with the solar wind at the magnetospheric boundary as the principal driving force. To the extent that their transpolar flow was concentrated at auroral zone latitudes, the observations presented here are consistent with the Axford and Hines model. However, we do not observe large-scale (>0.75 km/sec) convection directly across the polar cap as an ordinary feature of magnetospheric convection. Our experiment cannot determine whether weaker transpolar convection usually occurs.

Comparison with models of substorms and auroras. The short time scales we observe for major changes in the magnetospheric electric fields measured suggest ties with magnetic substorm phenomena. The same essential features of high-latitude convection, antisunward transpolar flow, and auroral-zone return paths appear in the magnetic substorm equivalent current systems derived by *Nishida* [1967], *Heppner* [1969], *Wescott et al.* [1969], and others, on the basis of ground magnetometer measurements. These currents are assumed to be concentrated in the ionosphere. *Oguti* [1969] similarly postulates antisunward transpolar flow on the basis of a three-dimensional model. It is possible that these substorm theories explain the transpolar flow observed in Figures 7 and 9, and the observed shifts in reversal latitude, since the substorm current pattern is presumably a transitory feature of the ionosphere.

A competing theory of magnetic substorms uses a three-dimensional current system with field-aligned currents [*Boström*, 1967; *Bonnevier et al.*, 1970, *Akasofu and Meng*, 1969]. A current is assumed to flow inward along a field line at dawn, through the ionosphere (auroral electrojet) from dawn to dusk, then outward along a dusk magnetic-field line. The effects of such field-aligned currents in the ionosphere were investigated theoretically by *Block and Fälthammar* [1968], thus leading to a theory of space-charge regions above auroras [*Carlqvist and Boström*, 1970]. A consequence of such a space-charge region is the existence of a current slab above the aurora containing a north-south electric field that reverses in the center of the slab. The fields will point toward the center if the field-aligned current is upward, and away from the slab center if the field-aligned current is downward. The electric fields are then presumed to cause $\mathbf{E}\times\mathbf{B}/B^2$ drifts. With the current system postulated, these drifts will be sunward at latitudes below the aurora and antisunward at higher latitudes. These fields and drifts are entirely consistent with our observations of the predominant directions of reversals. Carlqvist and Boström predict potentials at the center of the slabs of 10^3–10^5 volts, and this is consistent with the 3600- and 44,000-volt examples shown in Figures 8 and 10. If one assumes slab widths of 10^2–10^3 km, the range of convection velocities predicted encompasses the range of velocities observed.

Acknowledgments. We thank Dr. R. Sagalyn for providing electron number density data from the AFCRL experiment on Injun 5.

This research was supported in part by the National Aeronautics and Space Administration under contracts NAS5-10625, NAS1-8141, NAS1-8144(f), NAS1-8150(f), and NGL-16-001-043(97); and by the Office of Naval Research under contract N00014-68-A-0196-003.

* * *

The Editor thanks F. V. Coroniti and F. S. Mozer for their assistance in evaluating this paper.

REFERENCES

Akasofu, S.-I., and C.-I. Meng, A study of solar magnetic substorms, *J. Geophys. Res.*, *74*(1), 293–313, 1969.

Axford, W. I., Magnetospheric convection, *Rev. Geophys. Space Phys.*, *7*, 421–459, 1969.

Axford, W. I., and C. O. Hines, A unifying theory of high-latitude geophysical phenomena and geomagnetic storms, *Can. J. Phys.*, *39*, 1433, 1961.

Block, L. P., and C.-G. Fälthammar, Effects of field-aligned currents on the stucture of the ionosphere, *J. Geophys. Res.*, *73*(15), 4807–4812, 1968.

Bonnevier, B., R. Boström, and G. Rostocker, A three-dimensional model current system for polar magnetic substorms, *J. Geophys. Res.*, *75*(1), 107–122, 1970.

Boström, R., Auroral electric fields, in *Aurora and Airglow*, edited by B. M. McCormac, pp. 293–303, Reinhold, New York, 1967.

Carlqvist, P., and R. Boström, Space charge regions above the aurora, *J. Geophys. Res.*, *75*(34), 7140–7146, 1970.

Carpenter, D. L., Whistler studies of the plasmapause in the magnetosphere, 1, Temporal variations in the position of the knee and some evidence on plasma motion near the knee, *J. Geophys. Res., 71*(3), 693–709, 1966.

Carpenter, D. L., Whistler evidence of the dynamic behavior of the duskside bulge in the plasmasphere, *J. Geophys. Res., 75*(19), 3837–3847, 1970.

Carpenter, D. L., F. Walter, R. E. Barrington, and D. J. McEwen, Alouette 1 and 2 observations of abrupt changes in whistler rate and of VLF noise variations at the plasmapause: A satellite-ground study, *J. Geophys. Res., 73,* 2929, 1968.

Cauffman, D., A satellite study of dc electric field reversals in the magnetosphere, *Res. Rep. 71-15,* Univ. Iowa, Iowa City, 1971.

Cauffman, D., and D. Gurnett, Double probe measurements of dc electric fields with the Injun 5 satellite, *Res. Rep. 71-4,* Dep. Phys. Astron., Univ. Iowa, Iowa City, 1971.

Dungey, J. W., Interplanetary magnetic field and the auroral zone, *Phys. Rev. Lett., 6,* 47–48, 1961.

Fahleson, U. V., Theory of electric field measurements conducted in the magnetosphere with electric probes, *Space Sci. Rev., 7,* 238, 1967.

Fahleson, U. V., M. C. Kelley, and F. S. Mozer, Investigation of the operation of a dc electric field detector, *Planet. Space Sci., 18,* 1551–1561, 1970.

Föppl, H., G. Haerendel, L. Haser, R. Lüst, F. Melzner, B. Meyer, H. Neuss, H. Rabben, E. Rieger, H. Stocker, and W. Stoffregen, Preliminary results of electric field measurements in the auroral zone, *J. Geophys. Res., 73,* 21–26, 1968.

Gurnett, D. A., Satellite measurements of dc electric fields in the ionosphere, in *Particles and Fields in the Magnetosphere,* edited by B. M. McCormac, pp. 239–246, D. Reidel, Dordrecht, Netherlands, 1970.

Gurnett, D. A., G. W. Pfeiffer, R. R. Anderson, S. R. Mosier, and D. P. Cauffman, Initial observations of VLF electric and magnetic fields with the Injun 5 satellite, *J. Geophys. Res., 74*(19), 4631–4648, 1969.

Haerendel, G., and R. Lüst, Electric fields in the ionosphere and magnetosphere, in *Particles and Fields in the Magnetosphere,* edited by B. M. McCormac, pp. 213–228, D. Reidel, Dordrecht, Netherlands, 1970.

Haerendel, G., R. Lüst, and E. Reiger, Motion of artificial ion clouds in the upper atmosphere, *Planet. Space Sci., 15,* 1–18, 1967.

Heppner, J. P., Magnetospheric convection patterns inferred from high-latitude activity, in *Atmospheric Emissions,* edited by B. M. McCormac and A. Omholt, pp. 251–266, Van Nostrand Reinhold, New York, 1969.

Heppner, J. P., T. L. Aggson, and N. C. Maynard, The global distribution of electric field irregularities near 700 km, paper presented at Symp. Phys. Magnetosphere, Washington, D. C., September 1968.

Maynard, N. C., and J. P. Heppner, Variations in electric fields from polar orbiting satellites, in *Particles and Fields in the Magnetosphere,* edited by B. M. McCormac, pp. 247–253, D. Reidel, Dordrecht, Netherlands, 1970.

Mozer, F. S., and P. Bruston, Electric field measurements in the auroral ionosphere, *J. Geophys. Res., 72*(3), 1109–1114, 1967.

Mozer, F. S., and R. H. Manka, Magnetospheric electric field properties deduced from simultaneous balloon flights, *J. Geophys. Res., 76*(7), 1697–1712, 1971.

Mozer, F. S., and R. Serlin, Magnetospheric electric field measurements with balloons, *J. Geophys. Res., 74*(19), 4739–4754, 1969.

Nishida, A., Average structure and storm-time change of the polar topside ionosphere at sunspot minimum, *J. Geophys. Res., 72*(23), 6051–6061, 1967.

Oguti, T., Poleward travel of electric current filament in the polar cap region, *Rep. Ionos. Space Res., Jap., 23,* 175, 1968.

Piddington, J. H., A hydromagnetic theory of geomagnetic storms and auroras, *Planet. Space Sci., 9,* 947–957, 1962.

Potter, W. E., Rocket measurements of auroral electric and magnetic fields, *J. Geophys. Res., 75*(28), 5415–5431, 1970.

Taylor, H. A., Jr., H. C. Brinton, D. L. Carpenter, F. M. Bonner, and R. L. Heyborne, Ion depletion in the high-latitude exosphere; simultaneous Ogo 2 observations of the light ion trough and the VLF cutoff, *J. Geophys. Res., 74*(14), 3517–3528, 1969.

Van Allen, J. A., On the electric field in the earth's distant magnetotail, *J. Geophys. Res., 75*(1), 29–38, 1970.

Wescott, E. M., J. D. Stolarik, and J. P. Heppner, Electric fields in the vicinity of auroral forms from motions of barium vapor releases, *J. Geophys. Res., 74*(14), 3469–3487, 1969.

(Received January 28, 1971;
accepted May 21, 1971.)